Neutron-diffraction study of the Jahn-Teller transition in stoichiometric LaMnO₃

J. Rodríguez-Carvajal,* M. Hennion, F. Moussa, and A. H. Moudden

Laboratoire Léon Brillouin (CEA-CNRS), Centre d'Etudes de Saclay, 91191 Gif sur Yvette Cedex, France

L. Pinsard and A. Revcolevschi

Laboratoire de Chimie des Solides, Université Paris Sud, 91405 Orsay Cedex, France

The parent compound of the giant magnetoresistance Mn-perovskite, LaMnO₃, has been studied by thermal analysis and high-resolution neutron-powder diffraction. The orthorhombic *Pbnm* structure at room temperature is characterized by an antiferrodistorsive orbital ordering due to the Jahn-Teller effect. This ordering is evidenced by the spatial distribution of the observed Mn-O bond lengths. LaMnO₃ undergoes a structural phase transition at $T_{JT} \approx 750$ K, above which the orbital ordering disappears. There is no change in symmetry although the lattice becomes metrically cubic on the high-temperature side. The MnO₆ octahedra become nearly regular above T_{JT} and the thermal parameter of oxygen atoms increases significantly. The observed average cubic lattice is probably the result of dynamic spatial fluctuations of the underlying orthorhombic distortion. [S0163-1829(98)51706-7]

The oxides of perovskite structure containing Mn ions have recently been the object of a strong interest due to their exhibition of giant negative magnetoresistance effects.[1] Doping the family of compounds RMnO₃ (R: lanthanide) with divalent ions oxidizes Mn^{3+} to Mn^{4+}, introducing holes in the *d* band that give rise to a series of very interesting physical properties. The system of composition $La_{1-x}Ca_xMnO_3$ was studied some 40 years ago.[2,3] The parent compound LaMnO₃, is an antiferromagnetic insulator in which an orbital ordering is established due to the cooperative Jahn-Teller (JT) effect breaking the degeneracy of the electronic configuration of Mn^{3+} ($t_{2g}^3 e_g^1$). This particular orbital ordering is responsible for the *A*-type magnetic structure described in the remarkable experimental work by Wollan and Koehler.[3]

Hole doping increases the conductivity[2] and permits the ferromagnetic double-exchange interactions to produce ferromagnetic metals when doping is about $x=0.15$ to 0.35. Around $x=\frac{1}{2}$ charge-ordered states appearing at low temperatures[3] can be suppressed by the application of a magnetic field.[4] The understanding of the interplay between magnetic, transport, and structural properties in this family of compounds needs improved experimental microscopic data. These are necessary in order to test theories and to decipher the role of the different electronic processes taking place as a function of hole concentration, temperature, and structural features. One of the first models used to explain the magnetoresistance in the manganite perovskites was based on a Kondo lattice[5] where the double exchange and a strong Hund coupling play a fundamental role. Other theories argue that one of the main ingredients of the magnetoresistance physics is a strong electron-phonon interaction mediated by the JT effect.[6] Recently, the importance of this effect has been recognized in the formation of polaronic states.[7] It seemed, then, worthwhile studying in detail how the cooperative JT effect develops in stoichiometric LaMnO₃.

Powder samples of pure LaMnO₃ were prepared by crushing single-crystal ingots grown by the floating zone method.[8]

Such a procedure makes possible preparation of homogeneous composition polycrystalline materials. Differential thermal analysis (DTA) and thermogravimetric analysis (TGA) experiments were carried out in a SETARAM TGDTA 92-16 device in a temperature range of 20–1250 °C, experiments being performed under argon flow at a heating rate of 10 °C/min.

Two powder diffractometers of the Orphée Reactor at Laboratoire Léon Brillouin were used in this study. The diffractometer G4.2 for studying the behavior of the crystal structure as a function of temperature ($\lambda=2.59$ Å, $Q_{max}=4.2$ Å^{-1}, or $\lambda=1.99$ Å, $Q_{max}=6.2$ Å^{-1}) and the diffractometer 3T2 for refining the crystal structure with high direct space resolution ($\lambda=1.22$ Å, $Q_{max}=9.2$ Å^{-1}) at three selected temperatures below and above the phase transition. The program FullProf[9] was used to analyze the experimental data using the Rietveld method.

We have to point out that the synthesis conditions play an important role in defining the presence or absence of Mn^{4+} in the lattice. The first systematic study of the influence of firing atmosphere on the resulting unit cell of LaMnO₃ samples evidenced that when the percentage of Mn^{4+} is larger than 20%, the room temperature (RT) structure is rhombohedral.[10] The authors indicate the existence of an orthorhombic to rhombohedral phase transition at around 873 K for LaMnO₃ containing 2% Mn^{4+}. By increasing the Mn^{4+} concentration, the lattice distortion seems to diminish continuously. More recent structure determinations have been performed by Elemans *et al.*,[11] Tofield *et al.*,[12] van Roosmalen *et al.*,[13] Norby *et al.*,[14] Mitchell *et al.*,[15] and Huang *et al.*[16] These studies were mainly devoted to the study of defective LaMnO₃. The presence of Mn^{4+} is associated with the creation of cationic vacancies on both La and Mn sites.

The thermal analysis of our sample shows two transitions on heating. The first at $T_1=750$ K is evidenced by a sharp endothermic peak, which is not accompanied by a composition change, as shown by TGA data. The other transition is
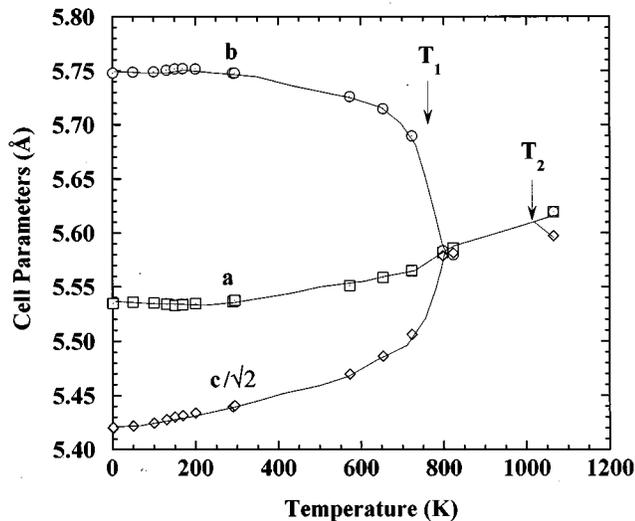
FIG. 1. Cell parameters of LaMnO$_3$ as a function of temperature. The continuous lines are a guide for the eyes. The "equivalent" $c/\sqrt{2}$ for the rhombohedral phase, $c_{eq} = c_O/\sqrt{2}$, is obtained from: $\mathbf{a}_H = \frac{1}{2}(\mathbf{a}_O - \mathbf{b}_O - \mathbf{c}_O)$, $\mathbf{b}_H = \mathbf{b}_O$, $\mathbf{c}_H = 2\mathbf{a}_O + \mathbf{c}_O$; so that $18c_{eq}^2 = c_H^2 + 12a_H^2$ (the subscripts H and O stand for hexagonal and orthorhombic, respectively).

indicated by a sharp endothermic peak at $T_2 = 1010$ K. Between the two transitions a continuous weight increase is observed. Above 1150 K a continuous weight loss is observed. It is worth mentioning that the temperatures for these phase transitions depend on the initial content of Mn^{4+}: the

sample used in Ref. 14 gave $T_1 = 600$ K and $T_2 = 800$ K, suggesting the presence of a non-negligble amount of Mn^{4+} that reduces the temperatures of the two phase transitions.

The analysis of powder diffraction patterns indicates that below T_1 the unit cell is orthorhombic and that between T_1 and T_2 the reflections can be indexed either assuming a double cubic perovskite or using a cell similar to the low-temperature orthorhombic cell. Above T_2, the compound becomes rhombohedral. The transition at T_1 is first order and hysteresis has been observed on cycling around T_1. The cell parameters as a function of temperature are represented in Fig. 1.

The first transition taking place at T_1 seems to be orthorhombic-to-cubic. Matsumoto announced the existence of this $O \rightarrow C$ transition in 1970.[17] Norby *et al.*[16] have performed a synchrotron x-ray diffraction study confirming this transition and the "cubic" character of the new phase. We shall see that the true symmetry of this phase is still orthorhombic. So the transition that we attribute to the suppression of the cooperative JT effect ($T_1 = T_{JT}$), does not change the average crystallographic symmetry. The refinement of the crystal structure below T_{JT} was performed using the $Pbnm$ space group. Above T_2, the space group $R\bar{3}c$ was used in the refinements.

In Table I we present some recent results published for the "stoichiometric" orthorhombic compound together with our results for three temperatures. A comparison of the published cell parameters indicates that a small presence of Mn^{4+} increases the c axis and diminishes the spontaneous orthorhombic strain $[s = 2(b-a)/(a+b)]$. A more distorted

TABLE I. Structural data of LaMnO$_3$ ($Pbmn$) at three selected temperatures. Data collection has been performed on the diffractometer 3T2, using a wavelength of 1.22 Å. The Jahn-Teller transition takes place at $T_{JT} = 750$ K. Cell parameters and atomic positions from references have been put in the $Pbnm$ setting. The representative atom positions of the asymmetric unit have been converted to those used in our work. The structural parameters described in the monoclinic space group $P2_1/n$ of Ref. 15 have been used to produce a simulated neutron diffraction pattern that has been refined using the $Pbnm$ space group (see text).

	RT	$T = 573$ K	$T = 798$ K	RT (Ref. 11)	RT (Ref. 14)	RT (Ref. 15)	RT (Ref. 16)
a (Å)	5.5367(1)	5.5520(2)	5.5817(3)	5.537(2)	5.5392(6)	5.5365(1)	5.5358(1)
b (Å)	5.7473(1)	5.7269(2)	5.5834(2)	5.743(1)	5.6991(7)	5.7216(1)	5.7363(1)
c (Å)	7.6929(2)	7.7365(2)	7.8896(4)	7.695(2)	7.7175(9)	7.7000(1)	7.6994(2)
x (La)	−0.0078(3)	−0.0063(3)	−0.0046(9)	−0.009(1)	−0.0063(7)	−0.0069(2)	−0.0080(3)
y (La)	0.0490(2)	0.0443(2)	0.0217(3)	0.050(1)	0.0435(5)	0.0459(2)	0.0475(3)
B (La)(Å^2)	0.34(2)	0.80(2)	1.26(3)				0.62(3)
B (Mn)(Å^2)	0.21(3)	0.46(4)	0.84(4)				0.51(6)
$x[O(1)]$	0.0745(3)	0.0725(3)	0.0687(10)	0.071(1)	0.0733(8)	0.0754(3)	0.0752(4)
$y[O(1)]$	0.4874(3)	0.4885(3)	0.4890(8)	0.489(1)	0.4893(8)	0.4883(3)	0.4869(4)
$B[O(1)](Å^2)$	0.50(3)	1.00(4)	1.87(7)				0.79(4)
$x[O(2)]$	0.7256(2)	0.7257(2)	0.7229(6)	0.725(1)	0.7257(6)	0.7262(2)	0.7256(3)
$y[O(2)]$	0.3066(2)	0.3038(2)	0.2831(5)	0.309(1)	0.3014(5)	0.3047(2)	0.3059(3)
$z[O(2)]$	0.0384(2)	0.0378(2)	0.0386(4)	0.039(1)	0.0385(4)	0.0384(1)	0.0385(2)
$B[O(2)](Å^2)$	0.43(3)	0.91(2)	1.67(5)				0.79(3)
R_p:	8.98	10.4	14.3			6.35	
R_{wp}:	9.04	10.0	11.3			9.97	
χ^2:	2.35	2.40	2.63			2.21	
$R_{Nucl}(\%)$:	5.16	5.32	4.14			2.82	
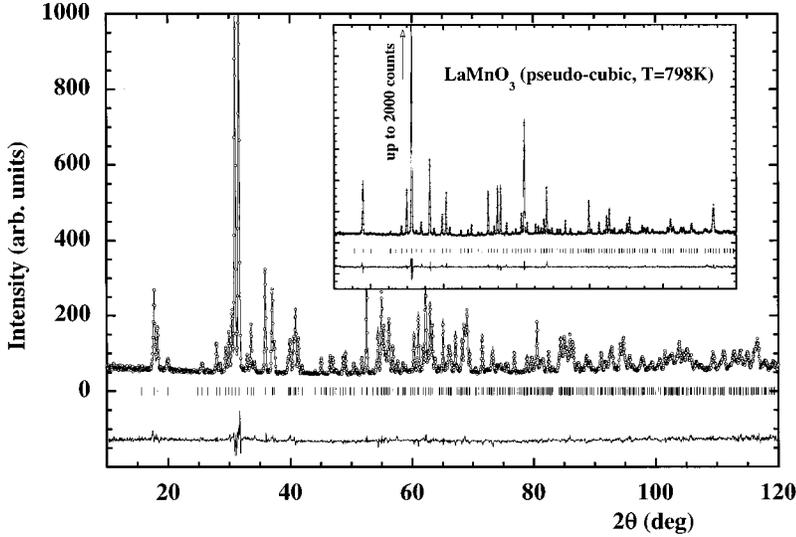
FIG. 2. Observed and calculated powder diffraction pattens of $LaMnO_3$ at $T=573$ K and at $T=798$ K (inset).

(monoclinic) phase has also been described for Mn^{4+}-free $LaMnO_3$.[15] In fact these data can also be refined within the orthorhombic system. We have performed a simulation using the structural parameters provided in Ref. 15 within the monoclinic space group $P2_1/n$ and profile parameters similar to those of our experimental conditions. Thermal parameters were kept fixed to arbitrary but physically sound values. A Poissonian noise was added to the calculated deterministic pattern and a Rietveld refinement, using the space group $Pbnm$, was carried out on the simulated data giving the results gathered in Table I.

Between T_{JT} and T_2, the full neutron diffraction profile can be fitted, without structural model, using a double cubic *primitive* unit cell. Taking into account the observed extinction conditions, the possible space groups are: $P23$, $P2_13$, $Pm\bar{3}$, $P432$, $P4_232$, $P\bar{4}3m$, $Pm\bar{3}m$, and $Pm\bar{3}n$. All of these groups were candidates to describe the crystal structure of

the high-temperature phase ($T_{JT}<T<T_2$) of $LaMnO_3$. In practice, none of them was successful in the refinement of the crystal structure of ''cubic'' $LaMnO_3$. The observed intensities of the Bragg reflections cannot be explained within the cubic symmetry. Actually no primitive cubic group was deduced by Glazer in his classification of rigid octahedra tilts in perovskites.[18] In fact, the refinement of the structure by using the low-temperature space group $Pbnm$ works perfectly. In Fig. 2, we have represented the observed and calculated diffraction patterns of $LaMnO_3$ below and above T_{JT}, obtained in the diffractometer 3T2.

In Table II we have also summarized the geometrical parameters that are directly related to the JT effect. The breaking of the degeneracy of e_g orbitals due to the JT effect can be described by the coefficients c_1 and c_2 determining the orbital occupation.[17,19] The temperature dependence of these coefficients is represented in Fig. 3.

TABLE II. Geometrical parameters characterizing the crystal structure of stoichiometric $LaMnO_3$ at three selected temperatures. The corresponding parameters at RT given in (or calculated from) various recent papers are also shown. The distortion parameter Δ of a coordination polyhedron BO_N with an average B-O distance $\langle d \rangle$, is defined as $\Delta=(1/N)\Sigma_{n=1,N}\{(d_n-\langle d \rangle)/\langle d \rangle\}^2$. The average tilt angle $\langle \varphi \rangle$ of MnO_6 octahedra around the pseudocubic [111] direction is obtained from the two superexchange angles θ_1 and θ_2 (see Ref. 20). The local modes characterizing the Jahn-Teller effect in $LaMnO_3$ defined as: $Q_2=2(l-s)/\sqrt{2}$ and $Q_3=2(2m-l-s)/\sqrt{6}$, where m, l, and s stand for medium, long, and short Mn-O distances. The bonding (Ψ_g) and antibonding (Ψ_e) orbitals are obtained as the linear combinations: $\Psi_g=c_1\phi_{x^2-y^2}+c_2\phi_{3z^2-r^2}$ and $\Psi_e=c_2\phi_{x^2-y^2}-c_2\phi_{3z^2-r^2}$. The coefficients c_1 and c_2 ($c_1^2+c_2^2=1$) can be obtained from the relations: $\tan\varphi=Q_2/Q_3$ and $\tan(\varphi/2)=c_1/c_2$ (see Refs. 17, 19).

	RT	$T=573$ K	$T=798$ K	RT (Ref. 11)	RT (Ref. 14)	RT (Ref. 15)	RT (Ref. 16)
Mn-O(1)×2(m)	1.9680(3)	1.9766(4)	2.010(1)	1.965(1)	1.973(1)	1.9706(3)	1.9708(4)
Mn-O(2)×2(s)	1.907(1)	1.914(2)	1.988(3)	1.901(6)	1.918(3)	1.9043(8)	1.907(2)
Mn-O(2)×2(l)	2.178(1)	2.164(2)	2.035(3)	2.189(6)	2.145(3)	2.1684(9)	2.174(2)
$\langle$Mn-O$\rangle$	2.0178(4)	2.0182(5)	2.011(1)	2.018(2)	2.012(1)	2.0144(3)	2.0171(6)
Δ(Mn-O)×10^{-4}	33.1	27.6	0.9	37.6	23.2	31.0	32.0
θ_1=Mn-O(1)-Mn	155.48(2)	156.13(2)	157.73(5)	156.6(1)	155.97(5)	155.28(1)	155.2(1)
θ_2=Mn-O(2)-Mn	155.11(5)	155.77(6)	157.9(1)	154.5(2)	155.9(1)	155.58(3)	155.4(8)
$\langle\varphi\rangle$	15.11	14.71	13.58	14.97	14.71	15.02	15.15
c_2	0.8074	0.7990	0.7148	0.8080	0.8021	0.7987	0.8023
$\langle$La-O$\rangle$	2.8174(5)	2.8179(6)	2.806(1)	2.818(2)	2.809(1)	2.812(1)	2.8156(7)
Δ(La-O)×10^{-4}	162.7	147.2	103.9	164.4	145.0	153.5	160.2
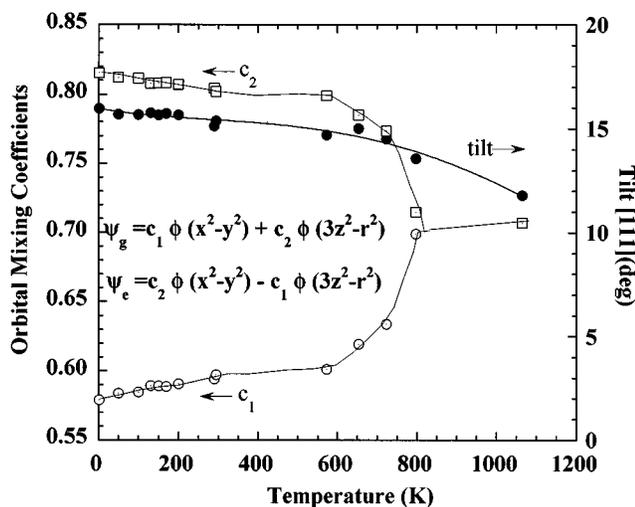
FIG. 3. Temperature dependence of the mixing coefficients c_1 and c_2 (see Table II), showing the disappearance of the static JT distortion above 750 K. The average tilt angle around the pseudocubic direction [111] is also displayed. The continuous lines are a guide for the eyes.

We observed that at T_{JT}, upon heating, *the orbital ordering disappears* (see Fig. 3). The orthorhombic O' phase becomes a special case of the orthorhombic O phase (a pseudocubic perovskite). The MnO_6 octahedra become much more regular but, as shown in Fig. 3, the tilt angle around the pseudocubic [111] axis is conserved. The average tilt angle has been calculated by taking the mean of the two tilts calculated from the geometrical relation given by O'Keefe and Hyde[20] as a function of the two superexchange angles $[\theta_1 = \text{Mn-O}(1)\text{-Mn}$ and $\theta_2 = \text{Mn-O}(2)\text{-Mn}]$. The absence of anomalous behavior in the average tilt angle shows that the transition taking place at T_{JT} is not simply related to steric effects. The presence of a primary electronic effect is clear: the distortion (see Δ in Table II) of the MnO_6 octahedra on going from the O' phase to the O phase diminishes drasti-

cally, indicating the disappearance of the static orbital ordering. The average Mn-O distance becomes smaller on heating at the transition and, then, remains nearly constant at higher temperatures $[\text{Mn-O}=2.008(2)$ at 1065 K in the rhombohedral phase].[21]

One of the problems to be addressed is to explain why the lattice is metrically cubic in the O phase. The most conventional explanation is that the "cubic" lattice results from a spatial averaging of microdomains of small orthorhombic distortion. This is a common situation found in several other perovskite systems that have been described as "double cubic" perovskites (see Ref. 22 and references therein). The case of $SrSnO_3$ (Ref. 22) is particularly instructive: high-resolution electron microscopy shows that crystals are formed by a three-dimensional multitwinning with the c axis of the *Pbnm* structure oriented in three perpendicular directions of the direct space.

If we calculate the cell parameters predicted by the O'Keefe-Hyde relations using the average Mn-O distance and tilt angle we obtain a significant difference between $c/\sqrt{2}$, a and b. The discrepancy is due to the nonrigidity of MnO_6 octahedra. The cubic metric could result from a subtle balance between tilt and octahedral nonrigidity, but the persistence of the cubic lattice of the O phase up to T_2 should involve fluctuations related to the dynamical JT effect. The picture is that in the high-temperature phase the local distortions of the MnO_6 octahedra are dynamics in character, and the system behaves as in the first case but with no static domains. A signature of that is the increase of the thermal factors of oxygen atoms in going from O' to the O phase. While the La and Mn atoms have an isotropic thermal factor varying linearly with temperature between RT and 798 K, oxygen atoms present an excess $\Delta B \approx 0.4$ Å^2 at the latter temperature. The orthorhombic symmetry persists in the O phase because the steric effects (Goldschmidt ratio tolerance factor) dominate: the average tilt angle does not change too much. At T_2 the change of symmetry towards the aristotype $(Pbnm \rightarrow R\bar{3}c \rightarrow Pm\bar{3}m)$ is driven by steric-thermal effects.

*Corresponding author. Electronic address: juan@bali.saclay.cea.fr

[1] R. von Helmolt *et al.*, Phys. Rev. Lett. **71**, 2331 (1993); Y. Tokura *et al.*, J. Phys. Soc. Jpn. **63**, 3931 (1994); S. Jin *et al.*, J. Appl. Phys. **76**, 6929 (1994).

[2] G. H. Jonker and J. H. Van Santen, Physica (Amsterdam) **16**, 337 (1950); **19**, 120 (1953); G. H. Jonker, *ibid.* **22**, 707 (1956).

[3] E. O. Wollan and W. C. Koehler, Phys. Rev. **100**, 545 (1955).

[4] Y. Tomioka *et al.*, Phys. Rev. Lett. **74**, 5108 (1995).

[5] N. Furukawa, J. Phys. Soc. Jpn. **63**, 3214 (1994).

[6] A. J. Millis *et al.*, Phys. Rev. Lett. **74**, 5144 (1995).

[7] H. Röder, J. Zang, and A. R. Bishop, Phys. Rev. Lett. **76**, 1356 (1996).

[8] A. Revcolevschi and R. Collongues, C.R. Séances Acad. Sci., Ser. A **266**, 1797 (1969); A. Revcolevschi, Rev. Int. Htes. Temps. **7**, 73 (1970).

[9] J. Rodríguez-Carvajal, Physica B **192**, 55 (1993).

[10] A. Wold and R. Arnott, J. Phys. Chem. Solids **9**, 176 (1959).

[11] J. B. A. A. Elemans *et al.*, J. Solid State Chem. **3**, 238 (1971).

[12] B. C. Tofield and W. R. Scott, J. Solid State Chem. **10**, 183 (1974).

[13] J. A. M. van Roosmalen *et al.*, J. Solid State Chem. **93**, 212 (1991); **110**, 100 (1994); **110**, 106 (1994).

[14] P. Norby *et al.*, J. Solid State Chem. **119**, 191 (1995).

[15] J. F. Mitchell *et al.*, Phys. Rev. B **54**, 6172 (1996).

[16] Q. Huang *et al.*, Phys. Rev. B **55**, 14 987 (1997).

[17] G. Matsumoto, J. Phys. Soc. Jpn. **29**, 606 (1970).

[18] A. M. Glazer, Acta Crystallogr., Sect. B: Struct. Crystallogr. Cryst. Chem. **28**, 3384 (1972); Acta. Crystallogr., Sect. A: Cryst. Phys., Diffr., Theor. Gen. Crystallogr. **31**, 756 (1975).

[19] J. Kanamori, J. Appl. Phys. **31**, 14S (1960).

[20] M. O'Keefe and B. G. Hyde, Acta Crystallogr., Sect. B: Struct. Crystallogr. Cryst. Chem. **33**, 3802 (1977).

[21] The refinement of the crystal structure of LaMnO$_3$ at 1065 K ($R\bar{3}c$) gives as a result in the hexagonal setting: $a=5.6196(3)$ Å, $c=13.6009(8)$ Å, La (6b) $B_{La}=2.1(2)$ Å^2, Mn (6a) $B_{Mn}=2.2(5)$ Å^2, O (18c) $x=0.5603(6)$, B$_O$=3.5(3) Å^2.

[22] A. Vegas *et al.*, Acta Crystallogr., Sect. B: Struct. Sci. **42**, 167 (1986).